

Extreme Memorization via Scale of Initialization

Harsh Mehta
Google
harshm@google.com

Ashok Cutkosky
Boston University
ashok@cutkosky.com

Behnam Neyshabur
Google
neyshabur@google.com

Abstract

We construct an experimental setup in which changing the scale of initialization strongly impacts the implicit regularization induced by SGD, interpolating from good generalization performance to completely memorizing the training set while making little progress on the test set. Moreover, we find that the extent and manner in which generalization ability is affected depends on the activation and loss function used, with sin activation being the most extreme. In the case of the homogeneous ReLU activation, we show that this behavior can be attributed to the loss function. Our empirical investigation reveals that increasing the scale of initialization could cause the representations and gradients to be increasingly misaligned across examples in the same class. We further demonstrate that a similar misalignment phenomenon occurs in other scenarios affecting generalization performance, such as changes to the architecture or data distribution.

1 Introduction

Large scale training of deep neural nets is the most successful modern recipe for building machine learning systems. As a result, there has been a significant interest in explaining some of the counter-intuitive behaviors seen in practice, with the end-goal of engendering further empirical success.

One such counter-intuitive trend is that the number of parameters in models being trained have increased considerably over time, and yet these models continue to increase in accuracy without loss of generalization performance. In practice, improvements can be observed even after the point where the number of parameters far exceed the number of examples in the dataset, i.e., when the network is overparametrized. These wildly over-parameterized networks avoid overfitting even without explicit regularization techniques such as weight decay or dropout, suggesting that the training procedure (usually SGD) has an implicit bias which encourages the net to generalize [Caruana et al., 2000, Neyshabur et al., 2014, 2019, Belkin et al., 2018a, Soudry et al., 2018].

In this paper, we examine the effect of *scale of initialization* on the generalization performance of SGD. While initialization is just a part of the training process, the literature already suggests that it may play an important role. Several initialization schemes have been proposed in order to facilitate neural network training from an optimization standpoint [Glorot and Bengio, 2010, He et al., 2015a]. Recent work explores some intriguing behavior induced by changing just the scaling of the net at initialization. Building on observation made by others [Li and Liang, 2018, Du et al., 2019, 2018, Zou et al., 2019, Allen-Zhu et al., 2018], [Chizat and Bach, 2018] formally introduces the notion of *lazy training*, a phenomenon in which an over-parametrized net can converge to zero training loss even as parameters barely change. [Chizat and Bach, 2018] further observes that any model can be pushed to this regime by scaling the initialization by a certain factor, assuming the output is close to zero at initialization. Moreover, [Woodworth et al., 2020] expands on how scale of initialization acts as a controlling quantity for transitioning between two very different regimes, called the kernel and rich regimes. In the kernel regime, the behavior of the net is equivalent to learning using kernel methods, while in the rich regime, gradient descent shows richer inductive biases which are not captured by RKHS norms. In practice, the transition from rich regime to kernel regime also comes with a drop in generalization performance. [Geiger et al., 2019] further explores interplay between hidden layer size

and scale of initialization in disentangling both regimes. In this work, we focus on studying the effect of scale of initialization from an empirical standpoint and observe that the extent and manner of the drop in generalization is dependent on the activation and loss function used, with ReLU activation being the most robust.

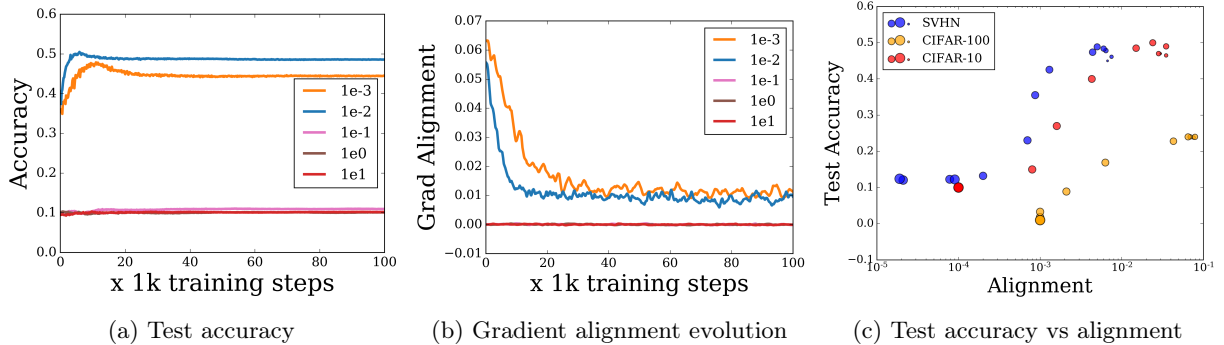


Figure 1: Results when using sin activation function in a 2-layer MLP. We initialize the first layer using random normal distribution with mean zero and vary the standard deviation σ as shown in the plots. Initialization scheme for the top layer is kept unchanged defaulting to glorot uniform initializer [Glorot and Bengio, 2010]. (a) shows the drastic changes in generalization ability solely due the changes in scaling on CIFAR-10 dataset. (b) shows how example gradients obtained after applying sin activation are increasingly misaligned as the scale of initialization is increased. Plot (c) shows the correlation between best test accuracy and gradient alignment values across 3 different datasets, CIFAR-10 [Krizhevsky, 2009] CIFAR-100 and SVHN.

Contributions In order to understand the interplay between training and generalization, we investigate situations in which the network can be made to induce an *extreme memorization* scenario in which the accuracy on the test set drops to random chance performance while attaining perfect accuracy on the training set. We have found that it is possible to construct an experimental setup in which simply changing the scale of the initial weights allows for a continuum of generalization ability, ranging from very little overfitting to perfectly memorizing the training set while making zero progress on test error.

- We construct a two-layer feed forward network with sin activation and observe that increasing the scale of initialization of the first layer strongly affects the implicit regularization induced by SGD, approaching complete memorization of the training set as the scale is increased. We observe this phenomenon on 3 different image classification datasets: CIFAR-10, CIFAR-100 and SVHN.
- In order to gain a better understanding of this phenomenon, we suggest an empirical “alignment” measure which can be used for both intermediate representations and gradients. We find that it correlates well with the generalization performance as the scale of initialization is increased and thus may help capture the inductive bias induced by SGD in these cases.
- Moving from sin to ReLU activation, we see a similar drop in generalization performance. Since ReLU is positive-homogenous, changing the scale should not affect the predictions of network with ReLU activation layers. We demonstrate that generalization behavior can be attributed further up in the network to a variety of common loss functions (softmax cross-entropy, hinge and squared loss). Further, this loss of generalization is accompanied by a corresponding decrease in gradient and representation alignment.
- Finally, we demonstrate that a similar misalignment phenomenon also occurs in other situations affecting generalization performance such as training on random labels instead of real data or inductive bias introduced by convolution and pooling operations, indicating that it might be of broader importance.

The rest of the paper is organized as follows. Sections 3 and 4 will primarily focus on the effect of the *scale of initialization* of the weights on the generalization performance. Specifically, for fixed activations functions,

architectures and datasets, we will alter the initial value of the weights provided to SGD by σ . In Section 3 we discuss the extreme memorization phenomenon which happens when we increase the scale of initialization while employing sin activation function. Inspired by observations from this construction, we define a measure of alignment across data points. Even though sin activation has started to enjoy more practical use recently [Sitzmann et al., 2020, Tancik et al., 2020], it is still less popular than other activation functions like ReLU and Sigmoid. We found sin activation to be most illustrative in exploring the connection between scale of initialization and generalization ability of neural nets due to its extreme behavior. However, these insights do carry over to more popular activation functions like ReLU, which we discuss in Section 4, and also why generalization performance is affected in that case despite its homogeneity property. Finally, in Section 5, we show that our alignment statistic is relevant in other well known scenarios concerning generalization in neural networks.

2 Related Work

Getting a clear handle on generalization performance of neural networks is a topic of widespread interest. In practice, while overparametrized nets generalize well when trained with SGD on real datasets, they can just as easily fit the training data when the labels are completely shuffled [Zhang et al., 2016], without changing anything else about the learning procedure. In fact, [Belkin et al., 2018b] show that the perfect overfitting phenomenon seen in deep nets can also be observed in kernel methods. Further studies like [Neyshabur et al., 2017, Arpit et al., 2017] expose the qualitative differences between the nets trained with real vs random data. These results suggest that nets do have the capacity to memorize all of the training data when left with no other choice. The generalization performance, in practice, is dependent on many factors including model family, number of parameters, learning rate schedule, explicit regularization techniques, batch size, etc [Keskar et al., 2016, Wilson et al., 2017]. [Xiao et al., 2019] further characterizes regions of hyperparameter spaces where the net memorizes the training set but fails to generalize completely.

Interestingly, there has been recent work showing that over-parametrization aids not just with generalization but optimization too [Du et al., 2019, 2018, Allen-Zhu et al., 2018, Zou et al., 2019]. [Du et al., 2018] shows that for sufficiently over-parameterized nets, the gram matrix of the gradients induced by ReLU activation remains positive definite throughout training due to parameters staying close to initialization. Moreover, in the infinite width limit the network behaves like its linearized version of the same net around initialization [Jacot et al., 2018]. They also explicitly characterize the solution obtained by SGD in terms of Neural Tangent Kernel which, in the infinite width limit, stays fixed through the training iterations and deterministic at initialization.

On a somewhat orthogonal direction, from a theoretical perspective, several studies attempt to bound the generalization error of the network based on VC-dimension [Vapnik, 1971], sharpness based measures such as PAC-Bayes bounds [McAllester, 1999, Dziugaite and Roy, 2017, Neyshabur et al., 2017], or norms of the weights [Bartlett, 1998, Neyshabur et al., 2015b, Bartlett et al., 2017, Neyshabur et al., 2019, Golowich et al., 2019]. Further works explore generalization from an empirical standpoint such as sharpness based measures [Keskar et al., 2016], path norm [Neyshabur et al., 2015a] and Fisher-Rao metric [Liang et al., 2017]. A few have also emphasized the role of distance from initialization in capturing generalization behavior [Dziugaite and Roy, 2017, Nagarajan and Kolter, 2019, Neyshabur et al., 2019, Long and Sedghi, 2019]. [Li and Liang, 2018] study 2-layer ReLU net and points out that final learned weights are accumulated gradients added to the random initialization and these accumulated gradients have low rank when trained on structured datasets. They observe that solutions learned by SGD on structured data are closer to initialization than unstructured data (random labels). Finally, noticing that many modern data-dependent techniques like Batch Normalization improves generalization performance, [Wei and Ma, 2019] obtains tighter bounds by considering data-dependent properties of the network such as norm of the Jacobians of each layer with respect to the previous layers. Our alignment statistic is also a data dependent measure which intuitively conveys a message similar to others that generalization performance depends on how similar representations and gradients are. Metrics based on example gradients have also been explored in similar recent studies such as Gradient Diversity [Yin et al., 2018], Gradient Confusion [Sankararaman et al., 2019] and Stiffness [Fort et al.,

2019]. Further, [Chatterjee, 2020] hypothesizes that similar examples lead to similar gradients, reinforcing each other in making the the overall gradient stronger in these directions and biasing the net to make changes in parameters which simultaneously benefit multiple examples.

3 Extreme memorization

In this section, we discuss the experimental setup which leads to extreme memorization due to increase in scale of initialization. In order to investigate this in the simplest setup possible, we consider a 2-layer feed-forward network trained using stochastic gradient descent (SGD):

$$z(x) = W_2 \phi(W_1 x)$$

where ϕ is the chosen activation function, $\mathbf{x} \in \mathbb{R}^p$, $\mathbf{W}_1 \in \mathbb{R}^{h \times p}$, $\mathbf{W}_2 \in \mathbb{R}^{k \times h}$ and $\mathbf{z} \in \mathbb{R}^k$ is the output of the net. The aim is to find model parameters $[\mathbf{W}_1^*, \mathbf{W}_2^*]$ which minimizes the empirical loss $\mathcal{L} = \frac{1}{n} \sum_{i=1}^n \ell(z(\mathbf{x}_i), \mathbf{y}_i)$ given i.i.d draws of n data points $\{(\mathbf{x}_1, \mathbf{y}_1) \dots (\mathbf{x}_n, \mathbf{y}_n)\}$ from some unknown joint distribution over $\mathbf{x} \in \mathbb{R}^p$ and $\mathbf{y} \in \mathbb{R}^k$. We focus on multi-class classification problems, in which each \mathbf{y} is restricted to be one of the standard basis vectors in \mathbb{R}^k . We will use the notation ℓ_i to indicate $\ell(\mathbf{z}(\mathbf{x}_i), \mathbf{y}_i)$ and $\mathbf{r}_i = \phi(\mathbf{W}_1 \mathbf{x}_i)$ as a short hand for the hidden layer representation for input \mathbf{x}_i . Also, for any $c \in \{1, \dots, k\}$, we will slightly abuse notation to write $y = c$ when indicating that \mathbf{y} is the c th standard basis vector.

Note that in our experiments, we choose a large hidden size so that the net is very over-parameterized and always gets perfect accuracy on the training set whenever possible. Also, since we are only interested in studying implicit regularization induced by SGD, we refrain from employing any of the commonly used explicit regularizers like weight decay, dropout, etc. More details on the experimental setup, datasets used and exact hyper-parameters can be found in the appendix.

3.1 Sin activation

As shown in Figure 1, setting ϕ to sin function results in a degradation of generalization performance arbitrarily to the point of complete memorization just by increasing the scale of initialization of the hidden layer W_1 . Intuitively, when using sin activations, if W_1 doesn't change a lot relative to its initialization value, then the output of a single hidden layer is a good approximation to the output of a kernel machine with a specific shift-invariant kernel K , where K is determined by the initializing distribution [Rahimi and Recht, 2008]. For example, when the initializing distribution is a Gaussian with standard deviation σ , K is a Gaussian kernel with width $1/\sigma$. Formally, consider a network architecture of $z(x) = W_2 \phi(W_1 x + b)$, where W_1 is a matrix whose entries are initialized via a Gaussian distribution with variance σ^2 and $b \in \mathbb{R}^h$ is a bias vector whose coordinates are initialized uniformly from $[0, 2\pi]$. Then [Rahimi and Recht, 2008] showed

$$\mathbb{E}_{W_1, b} [\langle \phi(W_1 x + b), \phi(W_1 x' + b) \rangle] \propto \exp\left(-\frac{\sigma^2 \|x - x'\|^2}{2}\right) \quad (1)$$

Thus, when holding W_1 and b fixed, the network approximates a kernel machine with a Gaussian kernel whose width decreases as the parameter W_1 is scaled up (which corresponds to increasing the variance parameter in its initialization). In this scenario, it is to be expected that the classifier will obtain near-perfect accuracy on the train data, but have no signal anywhere else because all points are nearly orthogonal in the kernel space. We did not specify a bias vector in our architecture, but intuitively one should expect similar behavior. In fact, we have the following analogous observation:

Theorem 1. *Suppose each entry of W_1 is initialized via a Gaussian with mean 0 and variance σ^2 . Then for any x and x' , we have*

$$\left| \mathbb{E}_{W_1} [\langle \phi(W_1 x), \phi(W_1 x') \rangle] \right| \leq h \exp\left(-\frac{\sigma^2 \|x - x'\|^2}{2}\right)$$

Proof. Since each individual row of W_1 is independent, it suffices to prove the statement for $h = 1$. If $x = 0$ the statement is trivially true, so suppose $x \neq 0$. Let $c = \frac{\langle x', x \rangle}{\|x\|^2}$ and let $\Delta = x' - cx$. Notice that $\langle \Delta, x \rangle = 0$ and $\|\Delta\| \leq \|x - x'\|$. We also have

$$W_1 x' = cW_1 x + W_1 \Delta$$

Notice that $W_1 x$ is normally distributed with mean 0 and variance $\sigma^2 \|x\|^2$. Further, $W_1 \Delta$ is normally distributed with mean 0 and variance $\sigma^2 \|\Delta\|^2$. Let A be a mean 0 random variable with variance $\sigma^2 \|x\|^2$ and B be a mean 0 random variable with variance $\sigma^2 \|\Delta\|^2$. Notice that since $\langle \Delta, x \rangle = 0$, the joint distribution $(W_1 x, W_1 x')$ is the same as that of $(A, cA + B)$. Therefore we have:

$$\begin{aligned} \left| \mathbb{E}_{W_1} [\langle \phi(W_1 x), \phi(W_1 x') \rangle] \right| &= \left| \mathbb{E}_{A,B} [\sin(A) \sin(cA + B)] \right| \\ &= |\mathbb{E}[\sin(A) \sin(cA) \cos(B) + \sin(A) \cos(cA) \sin(B)]| \\ &= |\mathbb{E}[\sin(A) \sin(cA) \cos(B)]| \\ &= |\mathbb{E}[\sin(A) \sin(cA)] \mathbb{E}[\cos(B)]| \\ &\leq |\mathbb{E}[\cos(B)]| \leq \exp\left(-\frac{\sigma^2 \|\Delta\|^2}{2}\right) \end{aligned}$$

□

This suggests that for large enough σ , the vectors $\phi(W_1 x)$ will be nearly uncorrelated in expectation at initialization. Further, for any loss function ℓ and label y , we have that the columns of $\nabla_{W_2} \ell(z(x), y)$ are proportional to $\phi(W_1 x)$, and so these gradients should also display a lack of correlation as σ increases. In this paper, we argue that this lack of correlation leads to memorization behavior.

Note that, by *memorization*, we mean that our trained model will have near-perfect accuracy on the training set, while having very low or even near-random performance on the testing set, indicating that the model has “memorized” the training set without learning anything about the testing set. To gain some intuition for why we might expect poor correlation among features or gradients to produce memorization, let us take a look at an extreme case where the gradients for all the examples are orthogonal to each other. More concretely, suppose the true data distribution is such that for all independent samples $(x_1, y_1), (x_2, y_2)$ with $(x_1, y_1) \neq (x_2, y_2)$, we have $\langle \nabla \ell_1, \nabla \ell_2 \rangle < \epsilon$ for all W_1, W_2 for some small ϵ . Then we should expect that taking a gradient step along any given example gradient should have a negligible $O(\epsilon)$ effect on the loss for any other example. As a result, the final trained model may achieve very small loss on the training set, but should learn essentially nothing about the test set - it will be a perfectly memorizing model.

3.2 Measuring Alignment

Motivated by this orthogonality intuition, we wish to develop a metric that can empirically measure the degree to which training points are in some sense well-aligned with each other. To begin with, we capture this by examining the gradient vectors. Our measure of alignment Ω between gradient vectors is defined as follows:

$$\Omega := \frac{\mathbb{E}_{i \neq j} [\langle \nabla \ell_i, \nabla \ell_j \rangle]}{\mathbb{E}[\|\nabla \ell\|^2]}$$

$$\text{Assuming } n \text{ vectors, } \mathbb{E}_{i \neq j} [\langle \nabla \ell_i, \nabla \ell_j \rangle] = \frac{\sum_{i \neq j} \langle \nabla \ell_i, \nabla \ell_j \rangle}{n(n-1)} \text{ and } \mathbb{E}[\|\nabla \ell\|^2] = \frac{\sum_{i=1}^n \|\nabla \ell_i\|^2}{n}$$

$$\Omega = \frac{n \sum_{i \neq j} \langle \nabla \ell_i, \nabla \ell_j \rangle}{(n-1)(\sum_{i=1}^n \|\nabla \ell_i\|^2)}$$

Note that $\sum_{i \neq j} \langle \nabla \ell_i, \nabla \ell_j \rangle$ may appear to require $O(n^2)$ time to compute, but in fact it can be computed in $O(n)$ time by reformulating the expressions as:

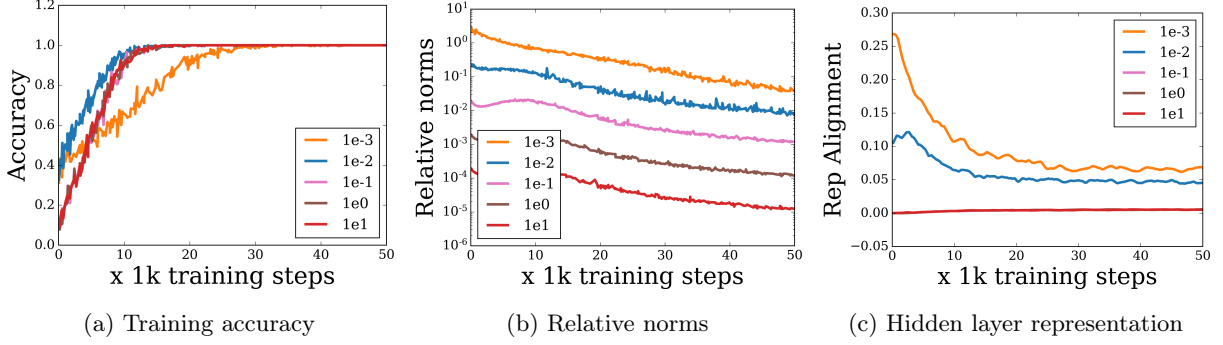


Figure 2: Results when using \sin activation function in a 2-layer MLP applied on CIFAR-10 dataset [Krizhevsky, 2009]. We initialize W_1 using random normal distribution with mean zero and vary the standard deviation σ as shown in the plots. Initialization scheme for W_2 is kept unchanged defaulting to glorot uniform initializer [Glorot and Bengio, 2010]. (a) shows the evolution and rate of attaining perfect training accuracy. (b) plots the norm of the gradients of W_1 over norm of W_1 . The lazy training phenomena elucidated in [Chizat and Bach, 2018] is present in the case of \sin activation as well. Plot (c) shows that representation alignment is also able to discriminate generalization ability induced at high scale of initialization. Finally, we obtain similar results on CIFAR-100 and SVHN datasets as well and are included in the appendix.

$$\sum_{i \neq j} \langle \nabla \ell_i, \nabla \ell_j \rangle = \left\| \sum_{i=1}^n \nabla \ell_i \right\|^2 - \sum_{i=1}^n \|\nabla \ell_i\|^2$$

Alignment within a class We formulate a class specific version as follows. For each class $c = 1, \dots, k$, we define:

$$\Omega_c := \frac{n_c \sum_{i \neq j} \langle \nabla \ell_i, \nabla \ell_j \rangle \mathbb{1}[y_i = y_j = c]}{(n_c - 1) (\sum_i \|\nabla \ell_i\| \mathbb{1}[y_i = c])^2}$$

where n_c is the number of training examples with label $y = c$ and $\mathbb{1}[p]$ is the indicator of the proposition p - it is one if p is true and zero otherwise. We further take the mean of Ω_c over all classes for an overall view of how in-class alignment behaves on average.

$$\Omega_{in-class} := \frac{1}{k} \sum_{c=1}^k \Omega_c$$

As shown in Figure 1, $\Omega_{in-class}$ correlates well with generalization ability of the net when scale of initialization is increased. **All of our gradient alignment plots report the average in-class alignment $\Omega_{in-class}$.**

Related gradient statistics Other relevant gradient-based measures have been suggested for understanding optimization or generalization. Figure 3 compares these measures against our alignment measure. Gradient diversity [Yin et al., 2018] defined as $\sum_{i=1}^n \|\nabla \ell_i\|_2^2 / \sum_{i=1}^n \|\nabla \ell_i\|_2^2$ is the most similar notion to alignment. However, as shown in Figure 3, Gradient Diversity is most sensitive when the cosine of the angle between two gradient is highly negative, a scenario which is rare in high dimensional spaces. Furthermore, this notation does not take the class information into account and treats all pairs of samples equally. We also observed that Gradient Diversity did not correlate with generalization in our experiments in Section 3. Cosine Gradient Stiffness [Fort et al., 2019] is another measure to capture the similarity of gradients and can be calculated as $\mathbb{E}_{i \neq j} [\cos(\nabla \ell_i, \nabla \ell_j)]$. [Fort et al., 2019] also define a modified version of Cosine Gradient Stiffness that allows this calculation within classes. As shown in Figure 3, this measure is invariant to the

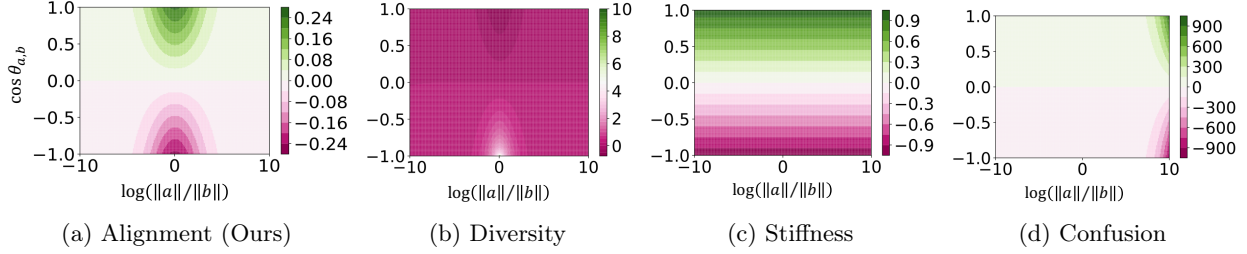


Figure 3: Comparing different gradient-based measures for the simple case of having two samples from the same class where $a = \nabla \ell_1$ and $b = \nabla \ell_2$.

scale of the gradient. That means that samples with very small gradients would be weighted as much as samples with large gradients, thus discarding valuable information. Therefore, our formulation of alignment measure normalizes by the **mean** gradient norm instead. Finally, gradient confusion [Sankararaman et al., 2019] can be calculated as $\min_{i \neq j} \langle \nabla \ell_i, \nabla \ell_j \rangle$. Figure 3 suggests that gradient confusion is very sensitive to the norm of gradients and is most affected by the ratio of the norms. Moreover, similar to Gradient Diversity, this measure does not take the class information into account.

Representation Alignment Since gradients are the sole contributor to changes in the the weights of the net, they play a crucial part in capturing generalization performance. However, note that gradients for W_2 are a functions of intermediate representations $r_i = \phi(W_1 x_i)$. Considering example representations instead of example gradients has a practical advantage that representations can be obtained for free with the forward pass but calculating gradients for every example in the batch can incur a significant compute and memory overhead. Also, representation alignment, defined below as Ω^r , at any training step, accounts for the cumulative changes made by the gradients since the beginning of the training where as gradient alignment only accounts for the current step. Thus, by the end of the training, as shown in Figure 2, we expect representation alignment to converge to a fixed value which can be used to compare changes in the network or hyper-parameters, regardless of the differences in training speed. Having said that, for completeness, we provide plots for both gradient and representation alignment for all the experiments where its useful to do so.

$$\Omega_{in-class}^r := \frac{1}{k} \sum_{c=1}^k \Omega_c^r \quad \Omega_c^r := \frac{n_c \sum_{i \neq j} \langle r_i, r_j \rangle \mathbb{1}[y_i = y_j = c]}{(n_c - 1) (\sum_i \|r_i\| \mathbb{1}[y_i = c])^2}$$

4 Why should the scaling affect homogeneous activations ?

In Section 3, we saw empirically that for a simple two-layer neural network with sin activations, we can induce a complete memorization scenario simply by increasing the scale of the initialization of the weights. For sin activations, this phenomenon may be explainable through the lens of random Fourier features and kernel machines, which suggests that large initialization leads to very poorly aligned examples. In this Section, we investigate what happens when we use more typical activations such as ReLU. We find that even for ReLU, increasing the scale of the initialization leads to a drop in generalization performance, and a similar downward movement in alignment as the initialization scale increases (see Figure 4). ReLU activation, due to its homogeneity property, should intuitively be robust to the scaling of initialization. However, this does not take into account the effect of the loss function ℓ , which is typically *not* homogeneous. We study 3 commonly used loss functions, namely softmax cross-entropy, multi-class hinge loss and squared loss, and show their effect on gradients when weights are close to their initialization. The result we present for ReLU holds for linear activation too. Even though with linear activations we don't expect the net to obtain perfect training accuracy, we do see the same trend in alignment measures and the drops in generalization performance that goes with it. Due to space constraints, we refer the reader to appendix Section E for the plots.

Note that increasing the scale of initialization also leads to the scale of the gradients being much smaller than the scale of the parameters at initialization [Chizat and Bach, 2018, Woodworth et al., 2020] and thus if it was high enough in the beginning, SGD should not be able to *fix* the scale of the weights during the course of the training.

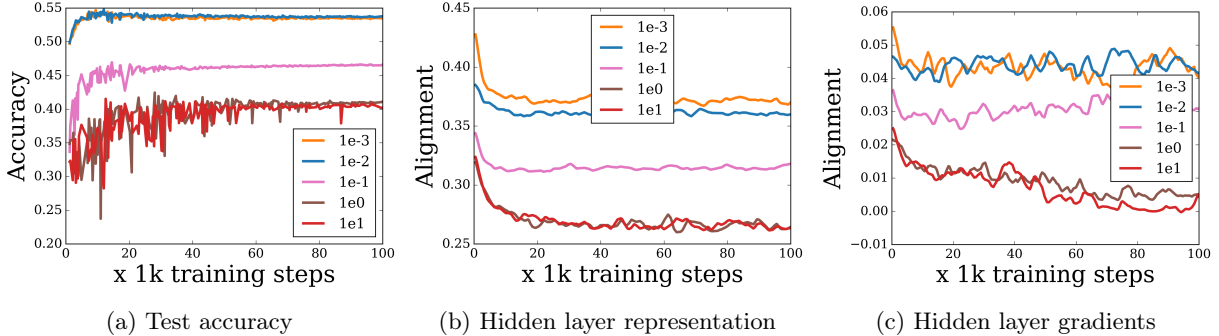


Figure 4: Results when using ReLU activation in a 2-layer MLP with Softmax cross-entropy loss function when trained on CIFAR-10 dataset. Similar to Figure 2, W_1 is initialized with random normal distribution with mean zero and varying standard deviation scale σ as shown in the plots. (a) shows how the test accuracy drops and saturates as σ is increased. (c) shows how gradients start to show misalignment as the scale is increased. (b) shows a similar misalignment trend for hidden layer representations. Note that, in contrast to the extreme memorization phenomenon we observed for sin activation, here we observe only a limited decrease in both generalization performance and alignment. Finally, similar results on CIFAR-100, SVHN and additional plots for CIFAR-10 with all the loss functions discussed in Section 4 can be found in the appendix.

Softmax cross entropy Typically, the softmax layer consists of a weight vector s_i for every class, which is used to compute the logits z_i . These logits then are used to compute the probability p_i for each class using the softmax function $g : \mathbb{R}^k \rightarrow \mathbb{R}^k$:

$$p_i = g_i(z) = \frac{e^{z_i/T}}{\sum_{j=1}^k e^{z_j/T}} \text{ for } i = 1, \dots, k \text{ and } z = (z_1, \dots, z_k) \in \mathbb{R}^k$$

Assuming T is 1, which is typically the case, observe that the derivative of the softmax with cross entropy with respect to the i th input z_i is

$$\frac{d}{dz_i} \ell(g(z), y) = p_i - y_i$$

where ℓ is the negative log-likelihood and $g(z) = (p_1, \dots, p_n)$ is the Softmax function. Let us consider the limiting behavior of this gradient when we increase the scale of the network, and consequently, the z values become arbitrarily high. In this case, all the p_i except the one corresponding to the largest z value become zero, so that the gradient is 0 if the prediction is correct, and otherwise is -1 in the coordinate of the correct class and 1 in the coordinate of the predicted class. Now, let us contrast this with the case where the scale of the network is arbitrarily close to 0. In this case, the gradient in the coordinate of the correct class will be $1/k - 1.0$ and $1/k$ in the incorrect class coordinates, so that all the gradients are the same and the alignment is 1, which is the maximum possible alignment. Therefore the gradients with respect to the logits will on average be more orthogonal in the former case. Since the gradients for parameters will be multiplied by gradient with respect to the logits due to the chain rule, they will be more orthogonal as well. We corroborate this intuition with empirical evidence as shown in Figure 4.

In practice, since the initialization scheme is chosen carefully, weight scaling is less of a concern in the beginning, but it can become an issue during the course of the training if the magnitude of the weights starts to increase. In either scenario, one simple strategy to counteract the effect of scaling of the net is to increase

the temperature term T with it such that magnitude of the input to the Softmax can stay the same and consequently there will be no relative change to alignment in the gradients coming from the loss function. Moreover, this observation also brings some clarity into why tuning hyper-parameters that affects the scale of the network is sometimes helpful in practice, either by explicitly tuning the temperature term or applying weight decay which favors parameters of low norm and implicitly controls the scale of the network throughout the training run.

Note that the arguments made for Softmax, which is typically used for multi-class classification, can also be adapted to Sigmoid for binary classification. Moreover, since Sigmoid is also used occasionally as an activation function, it is valuable to see how it behaves with changes in scale of initialization in that capacity. We do in fact observe similar degradation in generalization performance, although in this case, there is an extra complication that increasing the scale of the input to Sigmoid also affects the training accuracy since gradients for the hidden layer starts to saturate beyond a certain scale. More details on this can be found in the appendix.

Hinge loss In this case the overall loss is scaled with the scale of the network if we accept a smaller effective target margin. We define the hinge loss as:

$$\ell(z, y) = \sum_{i \neq y} \max(0, \Delta + z_i - z_y)$$

where Δ is the target margin. In practice Δ is typically set to 1.0. However, if the network outputs are scaled by a factor of α , this will have the same effect as scaling the margin to be $\frac{\Delta}{\alpha}$ and then scaling the loss by α : $\sum_{i \neq y} \max(0, \Delta + \alpha z_i - \alpha z_y) = \alpha \sum_{i \neq y} \max(0, \Delta/\alpha + z_i - z_y)$. With this in mind, let us calculate the gradient:

$$\frac{d\ell}{dz_i} = \begin{cases} \mathbb{1}(\Delta + z_i - z_y > 0) & i \neq y \\ -\sum_{i \neq y} \mathbb{1}(\Delta + z_i - z_y > 0) & i = y \end{cases}$$

It is instructive to take a look at what happens when the effective margin is arbitrarily close to zero. At initialization, we can treat each $\mathbb{1}(z_i - z_y > 0)$ as independently 0 or 1 uniformly at random, so we can expect half of the gradient coordinates for incorrect classes to be 1. On the other extreme, if the effective margin becomes large $\mathbb{1}(\Delta + z_i - z_y > 0)$ will always be 1, and the gradients for all incorrect classes will be 1. Again, the latter case will lead to the maximum alignment value of 1, so that the gradients more aligned across examples.

In this case, misalignment can be fixed by scaling the margin Δ with the scale of the network. Intuitively, we want to change the loss function such that the scale factor can be pulled out of the loss entirely so that scaling of the loss by a constant doesn't change the minimizer.

Squared loss

$$\ell(z, y) = \frac{1}{2}(z - y)^2$$

where y is a one hot vector with 1 in the coordinate of the correct class. The gradient with respect to z is $\frac{d\ell}{dz} = z - y$. In the extreme case where scale of the net is close to 0, z will also be close to zero so the y term will dominate in gradients for all the examples. On the other hand, when the scale is high, the z term dominates. Again, since y is a constant in our training and z will essentially be a random vector at initialization, we can expect the gradients across examples to be more aligned when the scale of the network is lower. Similar to the argument presented for hinge loss, the effect of scaling on generalization performance in this case can be fixed by scaling the one-hot vector y appropriately with it so that the scale factor can be pulled out of the loss function.

5 Is alignment relevant more broadly?

The preceding sections discuss how increasing the scale of initialization leads to a drop in gradient and representation alignment. This appears to shift the implicit bias induced by SGD towards directions that don't generalize as well. It is natural to wonder how prevalent this issue is. Said another way, changing the scale is only one way of causing the poor generalization performance, and it is possible that the alignment metric is simply correlated only with increasing scale rather than actually measuring anything about generalization. If we can find other ways to degrade generalization performance and those situations also lead to misalignment, this suggests that alignment is indeed more broadly relevant. In this Section, we take a look at such scenarios. More specifically, we are interested in knowing, is alignment relevant when we make changes to architecture or data distribution? We provide empirical evidence which suggests an optimistic answer in our exploration.

5.1 Inductive bias introduced by architecture changes

Introduction of new architecture changes has been a very successful recipe in advancing performance of deep learning models. In the task of image recognition, addition of convolutional layers and pooling layers [Lecun et al., 1998] and, more recently, residual layers [He et al., 2015b, 2016] have caused significant jumps in generalization performance. Moreover, several theoretical studies show how convolution and pooling operations can significantly affect the implicit bias of SGD, in favor of better generalization in the image domain [Cohen and Shashua, 2016, Gunasekar et al., 2018]. In Figure 5, we investigate the architectural change of extending our standard 2-layer MLP with preceding convolutional layers. Unsurprisingly, we observe substantial improvement in generalization performance. Moreover, the plots show that the addition of convolutional layers leads the last layer representations to be significantly more aligned suggesting that these architecture changes causes the net to discard irrelevant variations in the input more effectively across examples and ultimately leads to better generalization. Finally, we experiment with popular large scale image recognition models like ResNet-50 and DenseNet-121 [Huang et al., 2017] and also observe a similar trend.

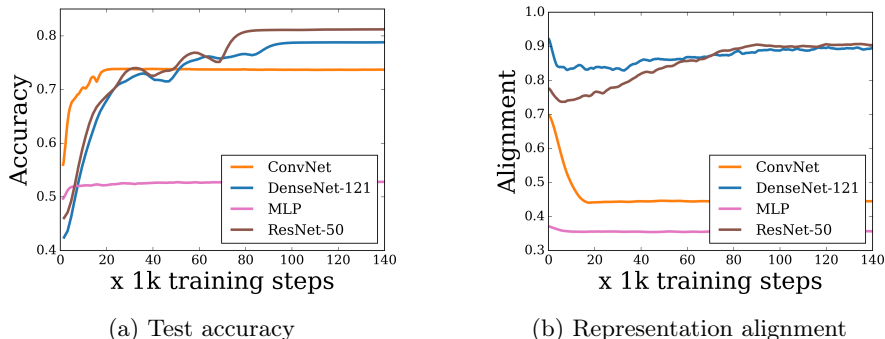


Figure 5: Comparison between 2-layer MLP with ReLU activation and a ConvNet architecture on CIFAR-10 dataset. Note that our ConvNet architecture is designed in such a way that last two layers are operationally the same as 2-layer MLP, including the hidden size and activation function. More details on this can be found in the appendix. As expected, ConvNet test accuracy is higher as shown in (a). Moreover, (b) suggests that the hidden layer representation are more aligned in the ConvNet architecture compared to 2-Layer MLP.

5.2 Changing the data distribution

Another way to strongly affect generalization performance is shuffling the labels in the training set, as popularized by [Zhang et al., 2016, Arpit et al., 2017]. If we completely shuffle the labels in the dataset, we don't expect the model to generalize on the test set at all, i.e., random chance performance. Moreover, Fig 6 shows that shuffling the labels also causes a drop in representational alignment. It is interesting to contrast the extreme memorization phenomenon introduced in Section 3 since in both cases we observe

random chance test accuracy while obtaining near-perfect train accuracy. The drop in alignment in Section 3 is more significant.

Even though the end result in generalization performance is the same, we believe these two scenarios are qualitatively quite different. In the case of varying initialization scale, we have changed something about the algorithm without modifying the data distribution. In the case of shuffled labels, we have instead in some sense made the problem “harder” by changing the data distribution (in a formal sense, we have increased the Bayes risk - no matter what regularization or implicit bias is present, it is unreasonable to expect the net to obtain good test accuracy).

Recall that our alignment metric is computed *for each class*. Intuitively, one would expect examples in the same class to be somehow similar and so therefore aligned in the input space. However, when we shuffle the labels, the class information becomes essentially worthless and as a result we may no longer see as much alignment among examples from a given class. Thus, alignment continues to be a reasonable proxy for the degree to which SGD finds generalizable patterns in the data, regardless of whether this degree is due to changes in the algorithm or changes in the distribution.

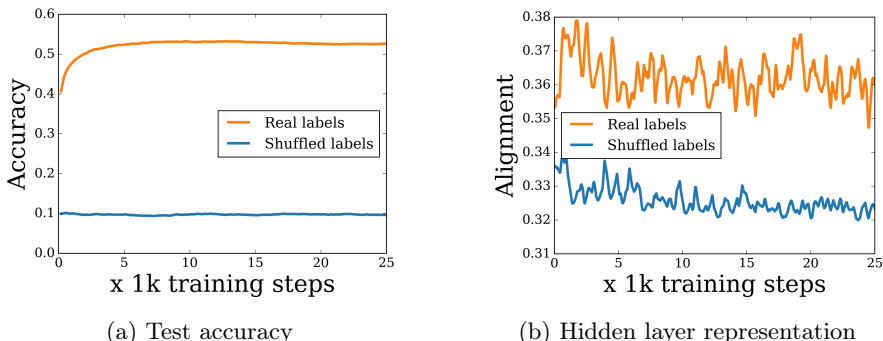


Figure 6: Comparing hidden layer representation alignment when a 2-layer MLP is trained on real labels from CIFAR-10 dataset, as opposed to when 100% of the labels are shuffled.

6 Conclusion and future work

We presented empirical evidence that scale of initialization alone can significantly alter generalization ability in neural nets for a variety of activation and loss functions. We observed an extreme case of this phenomenon in the case of sin activation, making it particularly interesting given a recent rise in the use of sin activation in practical setting [Sitzmann et al., 2020, Tancik et al., 2020]. This phenomena is also quite conspicuous even with more popular activations like ReLU and Sigmoid. Moreover, in the case of ReLU, we discovered that the loss function plays a crucial role since the rest of the net is unaffected by scaling due to homogeneity. In the case of Softmax cross-entropy, we also showed how the temperature term T is useful in canceling the effect of scale factors coming from the net. We complement these observations by defining an alignment measure that appears to correlate empirically well with generalization in a variety of settings.

Our formulation of alignment measure suggests some intriguing avenues for future research. For example, can we extend our metrics to capture changes in generalization performance when the number of hidden units is increased? Finally, as shown in Figure 1, even though our experiments suggest that low scale of initialization leads to increased representational alignment, there seems to be a sweet spot below which its affect on generalization ability no longer holds true. Exploring generalization behavior in this case of ultra-low scale of initialization is also an interesting direction of future research.

7 Acknowledgements

We are grateful to Eugene Ie and Walid Krichene for reading earlier drafts of this paper and providing valuable feedback.

References

- Zeyuan Allen-Zhu, Yuanzhi Li, and Zhao Song. A convergence theory for deep learning via over-parameterization, 2018.
- Devansh Arpit, Stanisław Jastrzębski, Nicolas Ballas, David Krueger, Emmanuel Bengio, Maxinder S. Kanwal, Tegan Maharaj, Asja Fischer, Aaron Courville, Y Bengio, and Simon Lacoste-Julien. A closer look at memorization in deep networks. 06 2017.
- P. L. Bartlett. The sample complexity of pattern classification with neural networks: the size of the weights is more important than the size of the network. *IEEE Transactions on Information Theory*, 44(2):525–536, 1998.
- Peter L Bartlett, Dylan J Foster, and Matus J Telgarsky. Spectrally-normalized margin bounds for neural networks. In *Advances in Neural Information Processing Systems*, pages 6240–6249, 2017.
- Mikhail Belkin, Daniel Hsu, Siyuan Ma, and Soumik Mandal. Reconciling modern machine learning practice and the bias-variance trade-off, 2018a.
- Mikhail Belkin, Siyuan Ma, and Soumik Mandal. To understand deep learning we need to understand kernel learning. 02 2018b.
- Rich Caruana, Steve Lawrence, and Lee Giles. Overfitting in neural nets: Backpropagation, conjugate gradient, and early stopping. In *Proceedings of the 13th International Conference on Neural Information Processing Systems*, NIPS’00, page 381–387, Cambridge, MA, USA, 2000. MIT Press.
- Satrajit Chatterjee. Coherent gradients: An approach to understanding generalization in gradient descent-based optimization, 2020.
- Lénaïc Chizat and Francis Bach. A note on lazy training in supervised differentiable programming. *ArXiv*, abs/1812.07956, 2018.
- Nadav Cohen and Amnon Shashua. Inductive bias of deep convolutional networks through pooling geometry, 2016.
- Simon S. Du, Jason D. Lee, Haochuan Li, Liwei Wang, and Xiyu Zhai. Gradient descent finds global minima of deep neural networks, 2018.
- Simon S. Du, Xiyu Zhai, Barnabas Poczos, and Aarti Singh. Gradient descent provably optimizes over-parameterized neural networks. In *International Conference on Learning Representations*, 2019. URL <https://openreview.net/forum?id=S1eK3i09YQ>.
- Gintare Karolina Dziugaite and Daniel M Roy. Computing nonvacuous generalization bounds for deep (stochastic) neural networks with many more parameters than training data. *arXiv preprint arXiv:1703.11008*, 2017.
- Stanislav Fort, Paweł Krzysztof Nowak, Stanisław Jastrzebski, and Sridhar Narayanan. Stiffness: A new perspective on generalization in neural networks, 2019.
- Mario Geiger, Stefano Spigler, Arthur Jacot, and Matthieu Wyart. Disentangling feature and lazy learning in deep neural networks: an empirical study. *ArXiv*, abs/1906.08034, 2019.

- Xavier Glorot and Yoshua Bengio. Understanding the difficulty of training deep feedforward neural networks. In Yee Whye Teh and Mike Titterton, editors, *Proceedings of the Thirteenth International Conference on Artificial Intelligence and Statistics*, volume 9 of *Proceedings of Machine Learning Research*, pages 249–256, Chia Laguna Resort, Sardinia, Italy, 13–15 May 2010. PMLR.
- Noah Golowich, Alexander Rakhlin, and Ohad Shamir. Size-independent sample complexity of neural networks. *Information and Inference: A Journal of the IMA*, May 2019. ISSN 2049-8764. doi: 10.1093/imaiai/iaz007. URL <http://dx.doi.org/10.1093/imaiai/iaz007>.
- Suriya Gunasekar, Jason Lee, Daniel Soudry, and Nathan Srebro. Implicit bias of gradient descent on linear convolutional networks, 2018.
- Kaiming He, X. Zhang, Shaoqing Ren, and Jian Sun. Delving deep into rectifiers: Surpassing human-level performance on imagenet classification. *2015 IEEE International Conference on Computer Vision (ICCV)*, pages 1026–1034, 2015a.
- Kaiming He, Xiangyu Zhang, Shaoqing Ren, and Jian Sun. Delving deep into rectifiers: Surpassing human-level performance on imagenet classification. *2015 IEEE International Conference on Computer Vision (ICCV)*, Dec 2015b. doi: 10.1109/iccv.2015.123. URL <http://dx.doi.org/10.1109/ICCV.2015.123>.
- Kaiming He, Xiangyu Zhang, Shaoqing Ren, and Jian Sun. Deep residual learning for image recognition. *2016 IEEE Conference on Computer Vision and Pattern Recognition (CVPR)*, Jun 2016. doi: 10.1109/cvpr.2016.90. URL <http://dx.doi.org/10.1109/cvpr.2016.90>.
- Gao Huang, Zhuang Liu, Laurens Van Der Maaten, and Kilian Q. Weinberger. Densely connected convolutional networks. *2017 IEEE Conference on Computer Vision and Pattern Recognition (CVPR)*, Jul 2017. doi: 10.1109/cvpr.2017.243. URL <http://dx.doi.org/10.1109/CVPR.2017.243>.
- Arthur Jacot, Franck Gabriel, and Clément Hongler. Neural tangent kernel: Convergence and generalization in neural networks, 2018.
- Nitish Shirish Keskar, Dheevatsa Mudigere, Jorge Nocedal, Mikhail Smelyanskiy, and Ping Tak Peter Tang. On large-batch training for deep learning: Generalization gap and sharp minima, 2016.
- Alex Krizhevsky. Learning multiple layers of features from tiny images. 2009.
- Alex Krizhevsky, Vinod Nair, and Geoffrey Hinton. Cifar-100 (canadian institute for advanced research). 2009. URL <http://www.cs.toronto.edu/~kriz/cifar.html>.
- Yann Lecun, Léon Bottou, Yoshua Bengio, and Patrick Haffner. Gradient-based learning applied to document recognition. In *Proceedings of the IEEE*, pages 2278–2324, 1998.
- Yuanzhi Li and Yingyu Liang. Learning overparameterized neural networks via stochastic gradient descent on structured data, 2018.
- Tengyuan Liang, Tomaso Poggio, Alexander Rakhlin, and James Stokes. Fisher-rao metric, geometry, and complexity of neural networks, 2017.
- Philip M. Long and Hanie Sedghi. Generalization bounds for deep convolutional neural networks, 2019.
- David A. McAllester. Pac-bayesian model averaging. In *Proceedings of the Twelfth Annual Conference on Computational Learning Theory, COLT '99*, page 164–170, New York, NY, USA, 1999. Association for Computing Machinery. ISBN 1581131674. doi: 10.1145/307400.307435. URL <https://doi.org/10.1145/307400.307435>.
- Vaishnavh Nagarajan and J. Zico Kolter. Generalization in deep networks: The role of distance from initialization, 2019.

- Yuval Netzer, Tiejie Wang, Adam Coates, Alessandro Bissacco, Baolin Wu, and Andrew Y. Ng. Reading digits in natural images with unsupervised feature learning. 2011.
- Behnam Neyshabur, Ryota Tomioka, and Nathan Srebro. In search of the real inductive bias: On the role of implicit regularization in deep learning, 2014.
- Behnam Neyshabur, Ruslan Salakhutdinov, and Nathan Srebro. Path-sgd: Path-normalized optimization in deep neural networks, 2015a.
- Behnam Neyshabur, Ryota Tomioka, and Nathan Srebro. Norm-based capacity control in neural networks. In *Conference on Learning Theory*, pages 1376–1401, 2015b.
- Behnam Neyshabur, Srinadh Bhojanapalli, David McAllester, and Nathan Srebro. Exploring generalization in deep learning, 2017.
- Behnam Neyshabur, Zhiyuan Li, Srinadh Bhojanapalli, Yann LeCun, and Nathan Srebro. The role of over-parametrization in generalization of neural networks. In *International Conference on Learning Representations*, 2019. URL <https://openreview.net/forum?id=BygfghAcYX>.
- Ali Rahimi and Benjamin Recht. Random features for large-scale kernel machines. In *Advances in neural information processing systems*, pages 1177–1184, 2008.
- Karthik Abinav Sankararaman, Soham De, Zheng Xu, W. Ronny Huang, and Tom Goldstein. The impact of neural network overparameterization on gradient confusion and stochastic gradient descent. *ArXiv*, abs/1904.06963, 2019.
- Vincent Sitzmann, Julien N.P. Martel, Alexander W. Bergman, David B. Lindell, and Gordon Wetzstein. Implicit neural representations with periodic activation functions. In *arXiv*, 2020.
- Daniel Soudry, Elad Hoffer, and Nathan Srebro. The implicit bias of gradient descent on separable data. In *International Conference on Learning Representations*, 2018. URL <https://openreview.net/forum?id=r1q7n9gAb>.
- Matthew Tancik, Pratul P. Srinivasan, Ben Mildenhall, Sara Fridovich-Keil, Nithin Raghavan, Utkarsh Singhal, Ravi Ramamoorthi, Jonathan T. Barron, and Ren Ng. Fourier features let networks learn high frequency functions in low dimensional domains. *arXiv preprint arXiv:2006.10739*, 2020.
- Vladimir Vapnik. Chervonenkis: On the uniform convergence of relative frequencies of events to their probabilities. 1971.
- Colin Wei and Tengyu Ma. Data-dependent sample complexity of deep neural networks via lipschitz augmentation, 2019.
- Ashia C Wilson, Rebecca Roelofs, Mitchell Stern, Nati Srebro, and Benjamin Recht. The marginal value of adaptive gradient methods in machine learning. In I. Guyon, U. V. Luxburg, S. Bengio, H. Wallach, R. Fergus, S. Vishwanathan, and R. Garnett, editors, *Advances in Neural Information Processing Systems 30*, pages 4148–4158. Curran Associates, Inc., 2017.
- Blake Woodworth, Suriya Gunasekar, Jason D. Lee, Edward Moroshko, Pedro Savarese, Itay Golan, Daniel Soudry, and Nathan Srebro. Kernel and rich regimes in overparametrized models, 2020.
- Lechao Xiao, Jeffrey Pennington, and Samuel S. Schoenholz. Disentangling trainability and generalization in deep learning. *ArXiv*, abs/1912.13053, 2019.

- Dong Yin, Ashwin Pananjady, Max Lam, Dimitris Papailiopoulos, Kannan Ramchandran, and Peter Bartlett. Gradient diversity: a key ingredient for scalable distributed learning. In Amos Storkey and Fernando Perez-Cruz, editors, *Proceedings of the Twenty-First International Conference on Artificial Intelligence and Statistics*, volume 84 of *Proceedings of Machine Learning Research*, pages 1998–2007, Playa Blanca, Lanzarote, Canary Islands, 09–11 Apr 2018. PMLR. URL <http://proceedings.mlr.press/v84/yin18a.html>.
- Chiyuan Zhang, Samy Bengio, Moritz Hardt, Benjamin Recht, and Oriol Vinyals. Understanding deep learning requires rethinking generalization. *CoRR*, abs/1611.03530, 2016. URL <http://arxiv.org/abs/1611.03530>.
- Difan Zou, Yuan Cao, Dongruo Zhou, and Quanquan Gu. Gradient descent optimizes over-parameterized deep relu networks. *Machine Learning*, 109(3):467–492, Oct 2019. ISSN 1573-0565. doi: 10.1007/s10994-019-05839-6. URL <http://dx.doi.org/10.1007/s10994-019-05839-6>.

A Organization of the appendix

- We describe the training procedure and datasets used throughout the paper in detail in appendix B.
- In appendix C, we reproduce the extreme memorization phenomenon from Figure 2 on CIFAR-100 and SVHN.
- In Section 4, Fig 4 shows how changing the scale of activation leads to a drop in generalization performance in the case of ReLU activation and softmax cross-entropy loss. In appendix D, we include results with multi-class hinge and squared losses.
- We include results when using linear activation with softmax cross-entropy loss in appendix E.
- In appendix F, we discuss how Sigmoid function, when used as activation, responds to scaling of initialization.
- Appendix G includes details on the exact architecture and hyperparameters used for the convolutional net in Section 5.1.

B Description of the training procedure and datasets

We use the Tensorflow framework for conducting our empirical study and all of our code is included as part of supplementary material. In every experiment, we train using SGD, without momentum, with a constant learning rate of 0.01 and batch size of 256. We employ a p100 single-instance GPU for each training run. For most of the experiments, the model is trained until it obtains perfect accuracy on the training set, with only a few exceptions which are either unavoidable or requires extravagant training iterations. For example, in the experiments involving linear activation, since none of the datasets we use are completely linearly separable, we do not expect the net to get 100% accuracy on the training set. Another interesting case is the Sigmoid activation, for which the gradients starts to saturate as the scale of the input to the Sigmoid function increases. Thus, we stop the training at a point when at least one of the model in the study achieves perfect accuracy on the training set.

In our 2-layer MLP model, in almost all cases we use 1024 units for the hidden layer with exceptions of 1) experiments with Sigmoid activation and 2) ReLU activation with squared loss. In both of these cases, we increase the number of hidden units to 2048 in order to increase their training speed. Number of units for the softmax layer depends on the number of output classes, which is 10 for CIFAR-10 / SVHN, and 100 for CIFAR-100. The details of the ConvNet architecture are included in appendix G. For any layer that doesn't involve changing the initialization scale, for instance the top layer in all our models, defaults to using Glorot uniform initializer [Glorot and Bengio, 2010]. For experiments corresponding to Sections 3 and 4, we refrain from employing bias variables in order to match the setup exactly. For experiments in Section 5, all biases are initialized to zero.

We employ 3 image classification datasets each having 32x32 pixels color image as input. CIFAR-10 dataset [Krizhevsky, 2009] consists of 60000 images with 10 classes. Classes are balanced with 6000 images per class. Training set consists of 50000 images and 10000 test images. CIFAR-100 [Krizhevsky et al., 2009] is very similar to CIFAR-10 except that it has 100 classes with 600 images per class. Finally, The Street View House Numbers (SVHN) Dataset [Netzer et al., 2011] has images of digits from house numbers obtained from Google Street View with a total of 10 classes. Training set contains 73257 images and 26032 test images.

C Sin activation

Figure 2 shows that increasing the scale of initialization for hidden layer weights W_1 in a 2-layer MLP model leads to extreme memorization on CIFAR-10 dataset. Keeping everything else the same, we reproduce the same phenomenon on two other datasets, namely, CIFAR-100 and SVHN respectively.

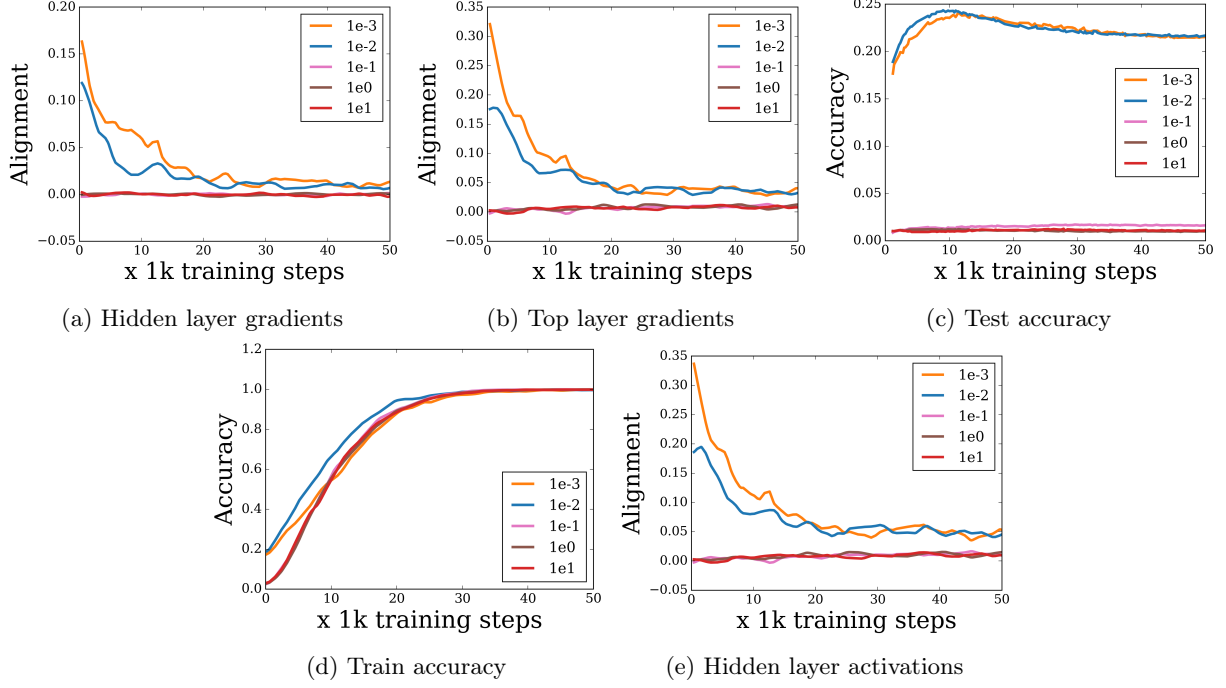


Figure 7: Results when using sin activation function on CIFAR-100 dataset.

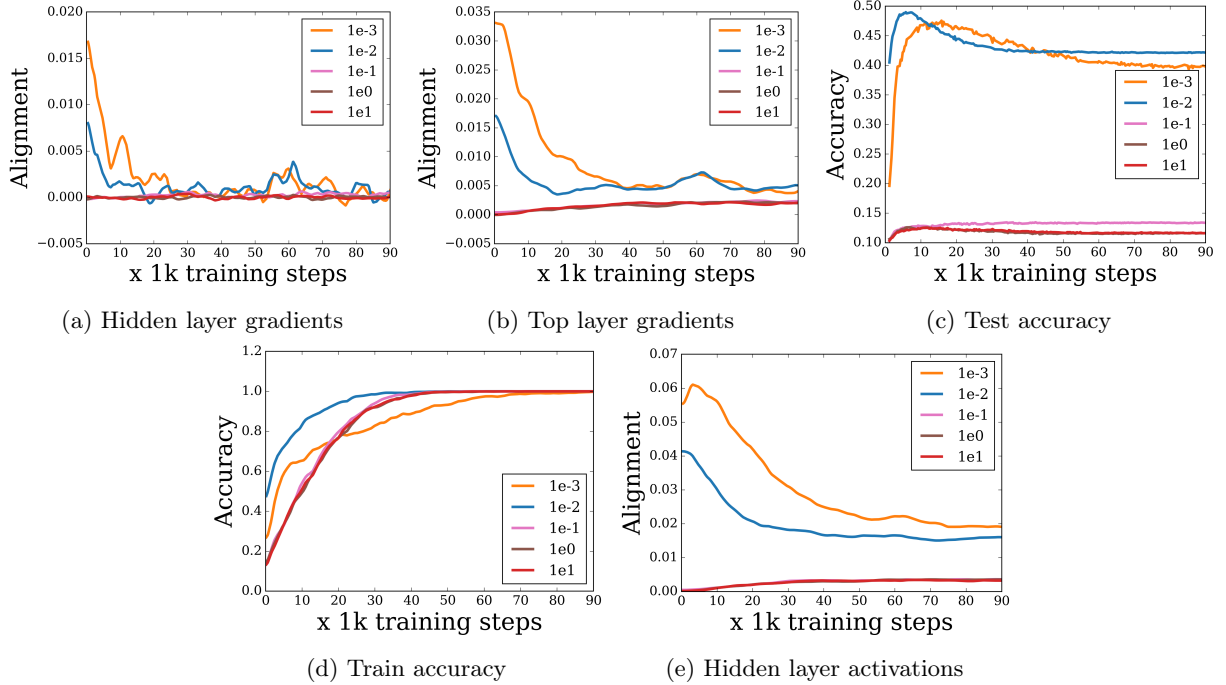


Figure 8: Results when using sin activation function on SVHN dataset.

D ReLU activation

D.1 Softmax cross entropy

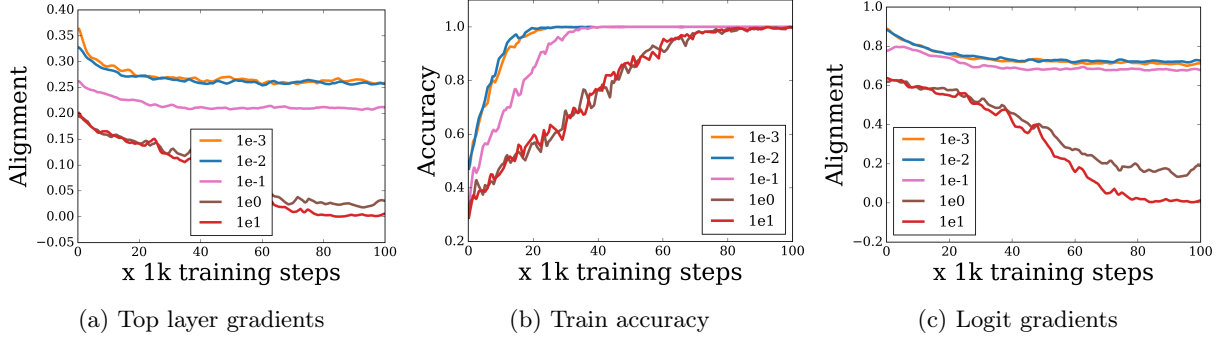


Figure 9: Additional plots when using ReLU activation function with softmax cross-entropy on CIFAR-10 dataset.

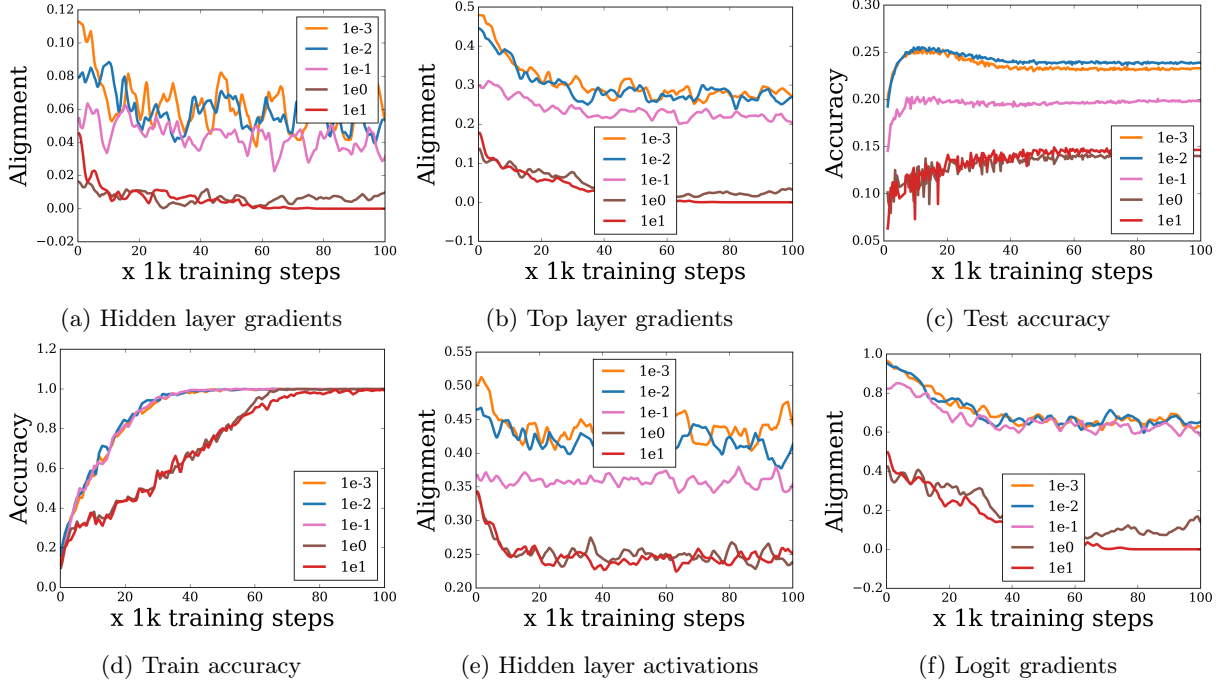


Figure 10: Results when using ReLU activation function with softmax cross-entropy on CIFAR-100 dataset.

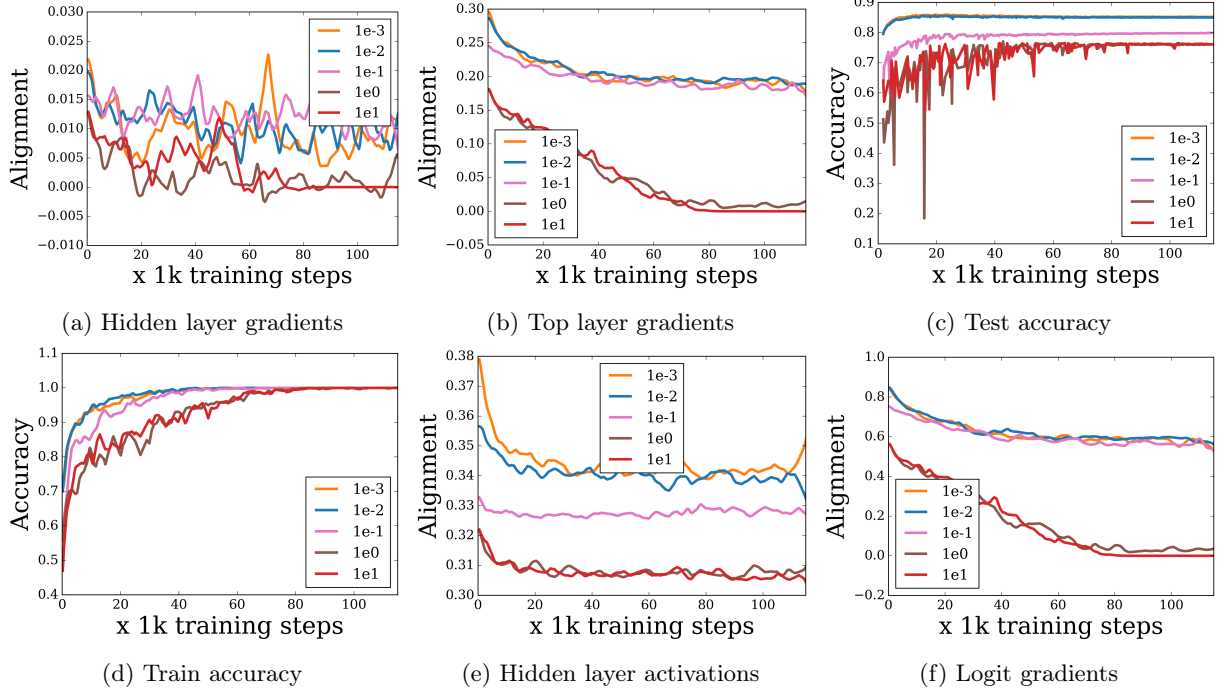


Figure 11: Results when using ReLU activation function with softmax cross-entropy on SVHN dataset.

D.2 Hinge loss

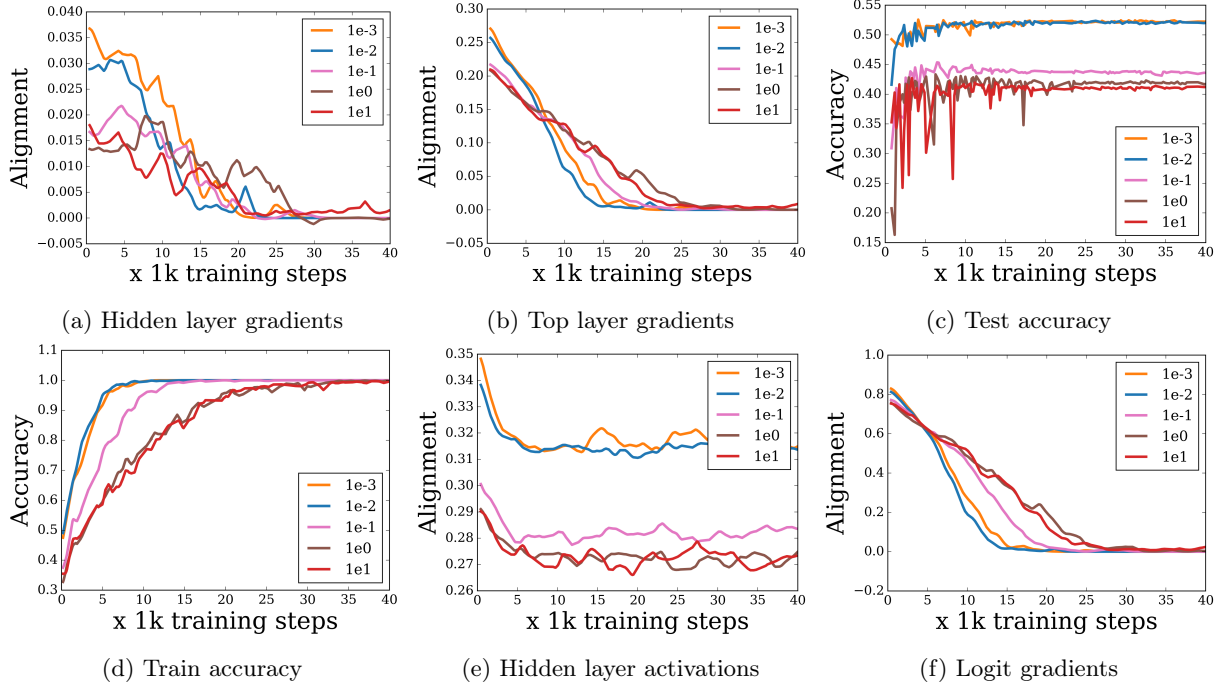


Figure 12: Results when using ReLU activation function with hinge loss on CIFAR-10 dataset.

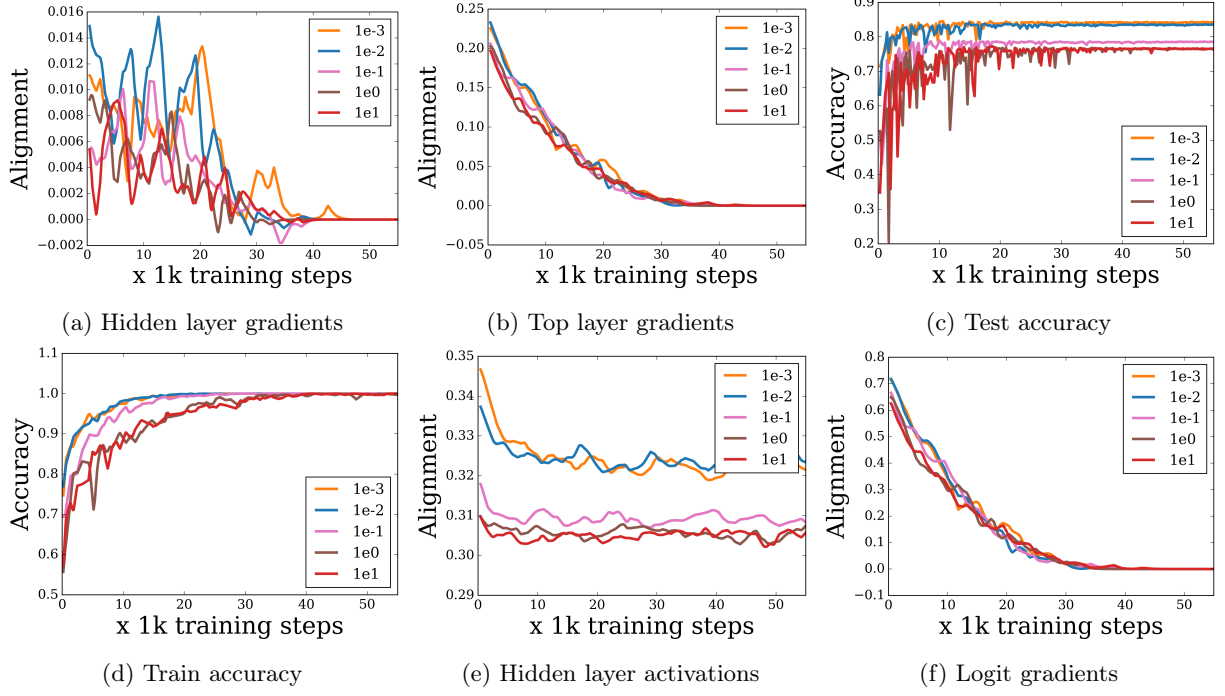


Figure 13: Results when using ReLU activation function with hinge loss on SVHN dataset.

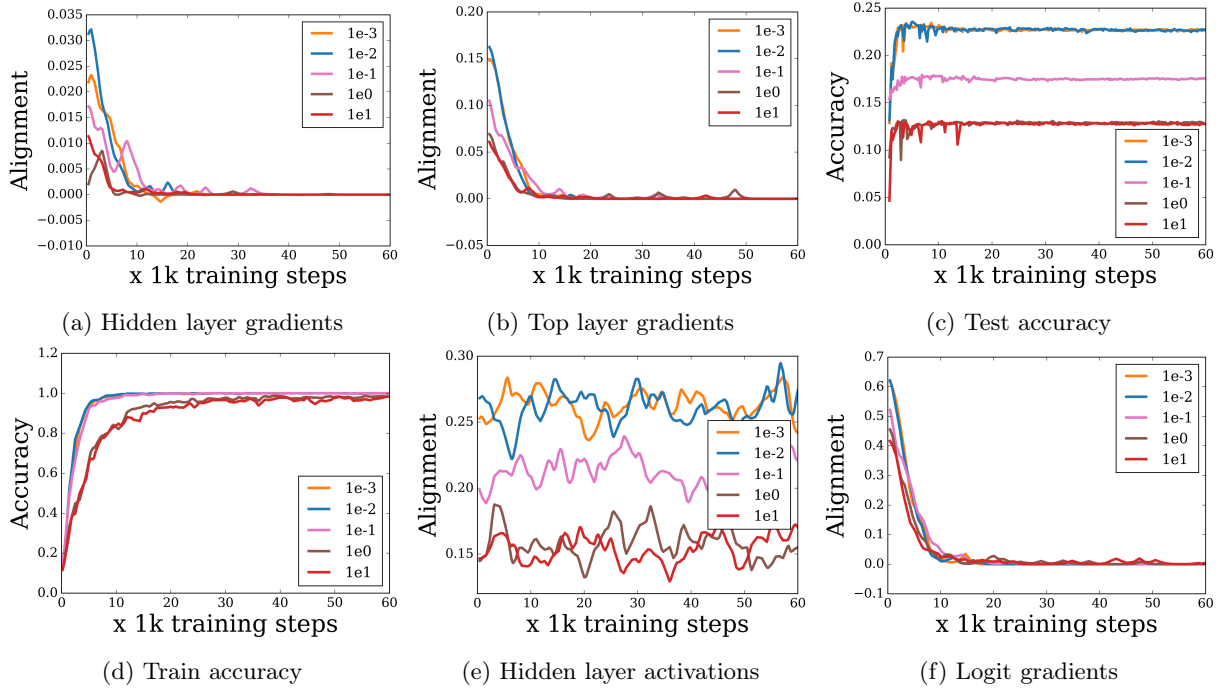


Figure 14: Results when using ReLU activation function with hinge loss on CIFAR-100 dataset.

D.3 Squared loss

Note that when employing squared loss, we increase the number of hidden units from the usual 1024 units to 2048 in order to compensate for very low training speed. Also, we observed that increasing the scale of initialization for W_1 beyond a certain scale leads to divergence in training after a few iterations. Thus, we recover the phenomenon of interest with much less aggressive increase in scale of initialization i.e. we double the standard deviation instead of increasing it by ten times as done in other experiments.

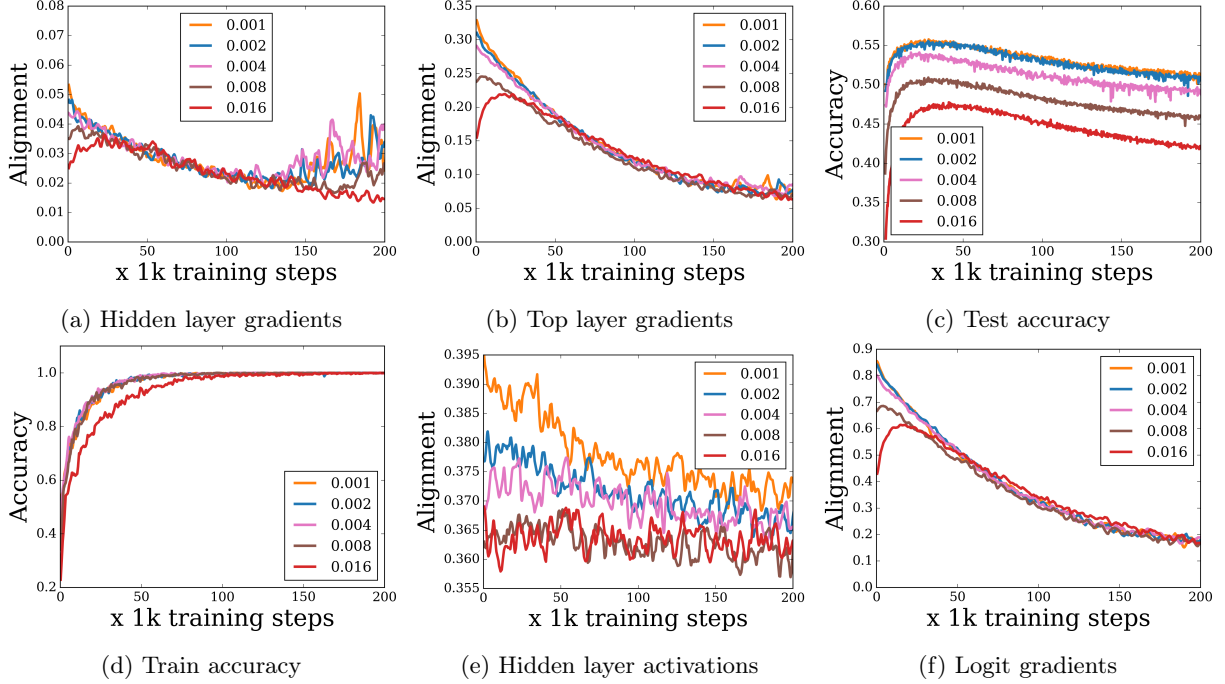


Figure 15: Results when using ReLU activation function with squared loss on CIFAR-10 dataset.

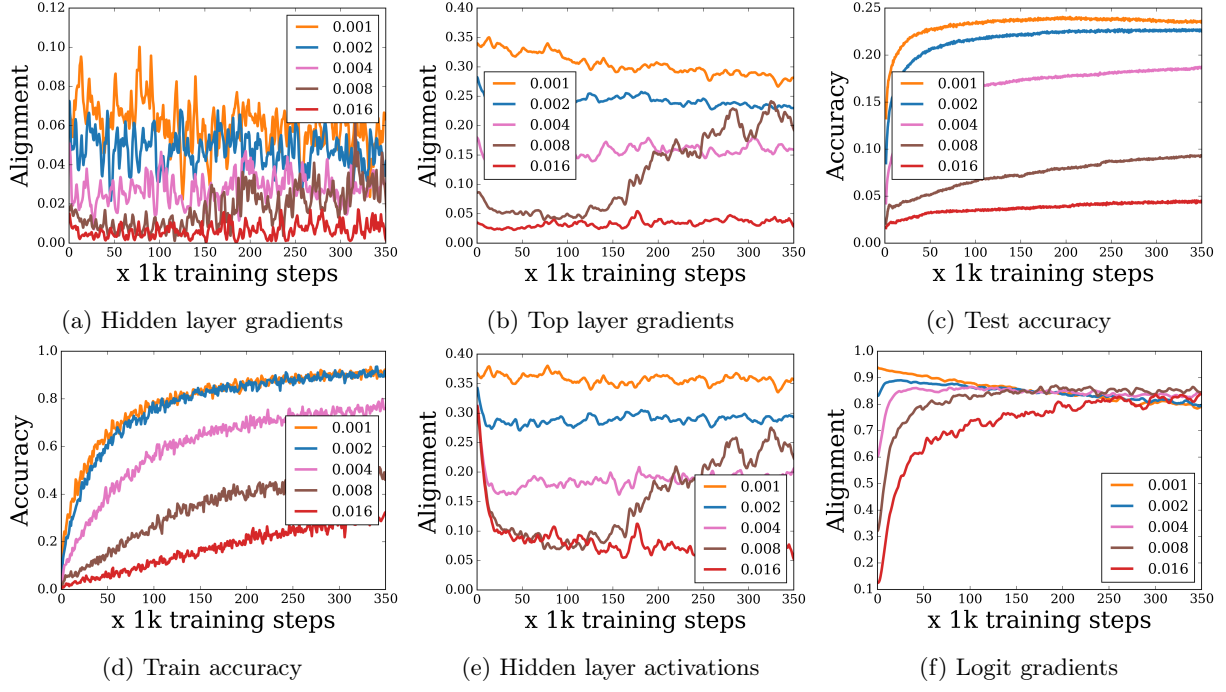


Figure 16: Results when using ReLU activation function with squared loss on CIFAR-100 dataset.

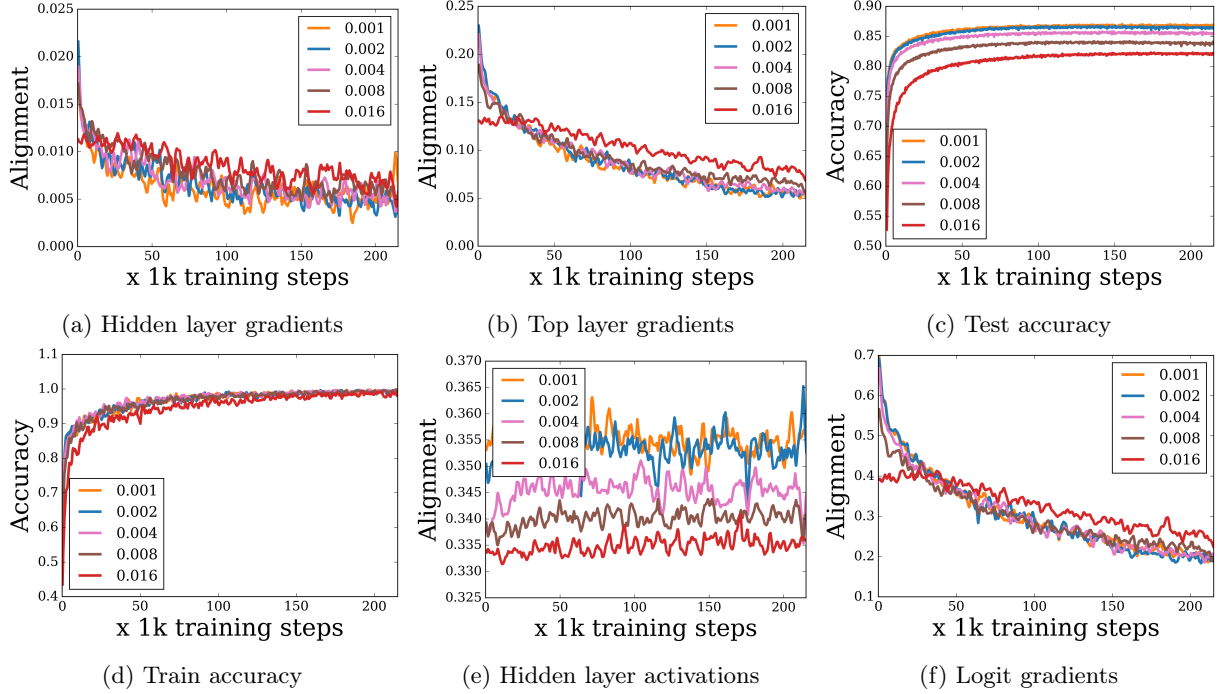


Figure 17: Results when using ReLU activation function with squared loss on SVHN dataset.

E Linear activation

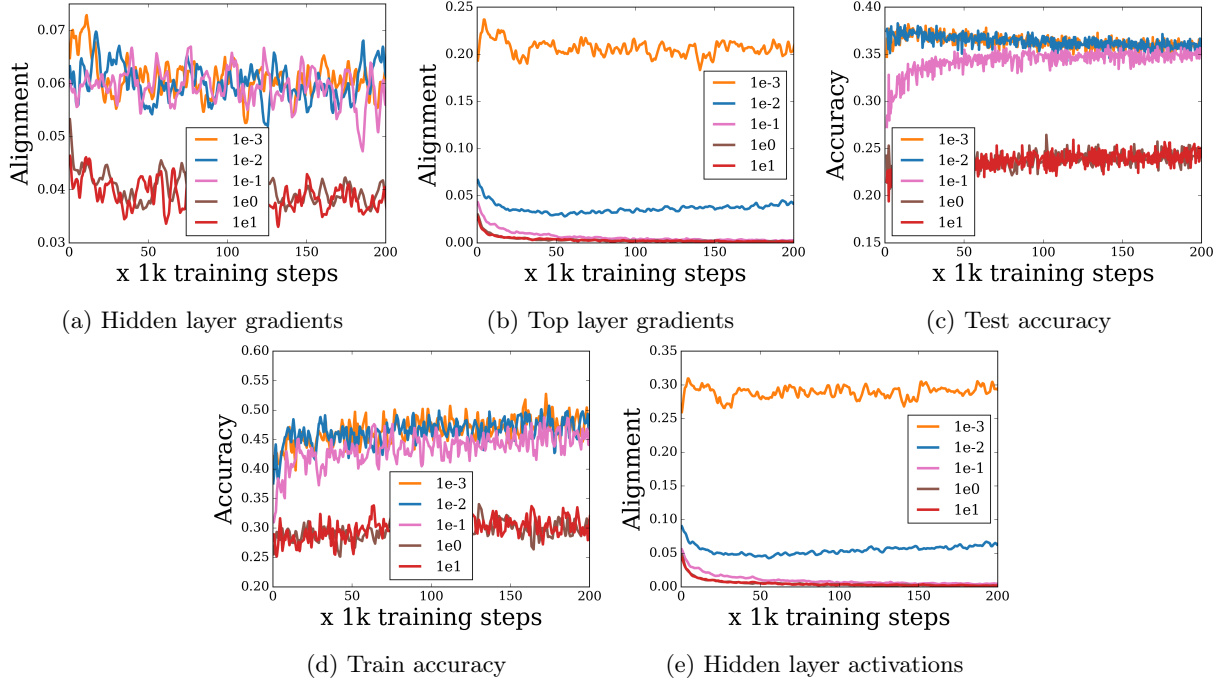


Figure 18: Results when using linear activation function with softmax cross entropy loss on CIFAR-10 dataset.

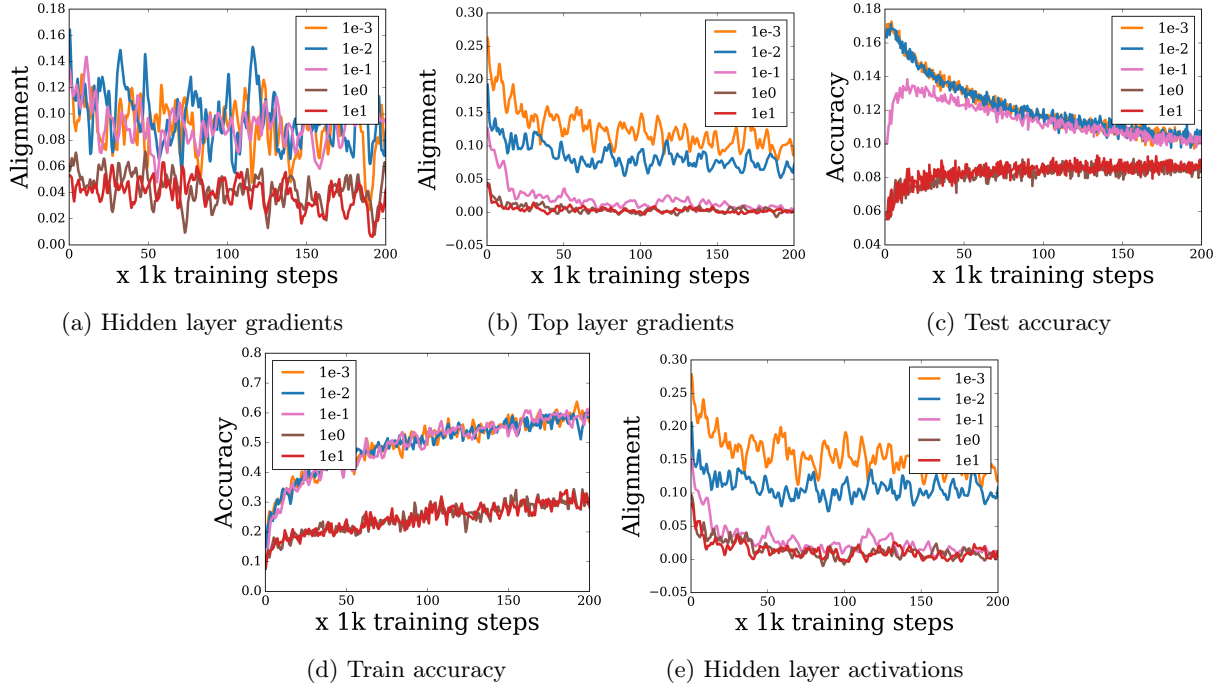


Figure 19: Results when using linear activation function with softmax cross entropy loss on CIFAR-100 dataset.

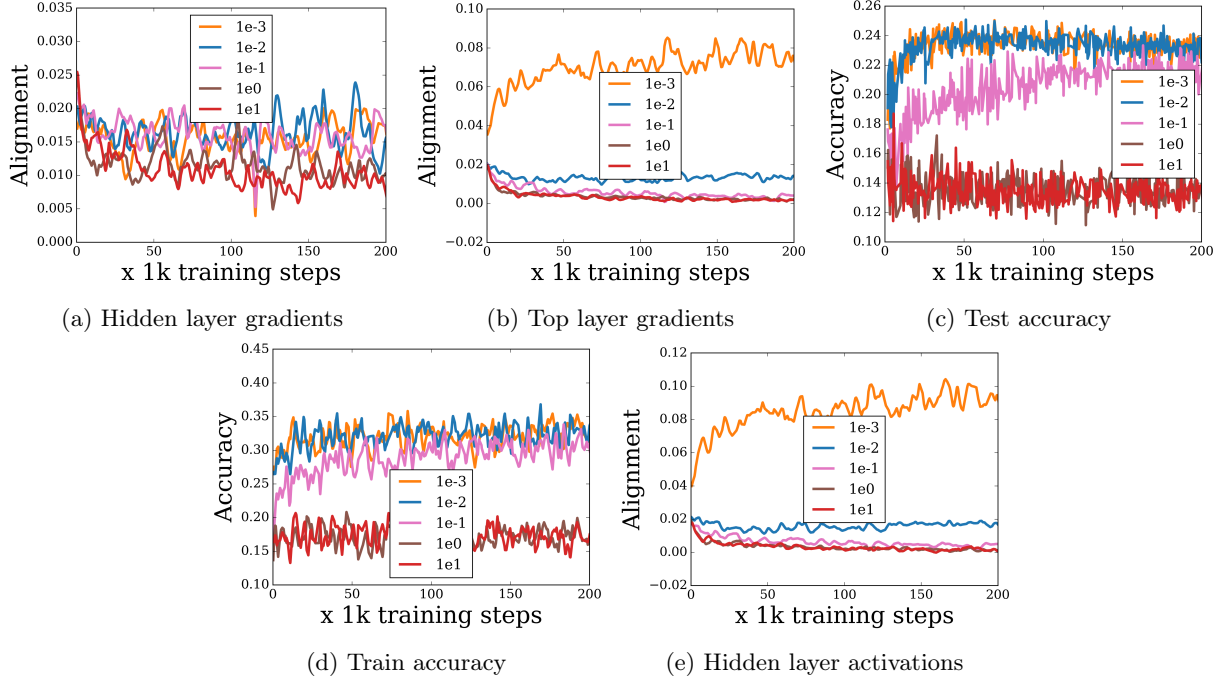


Figure 20: Results when using linear activation function with softmax cross entropy loss on SVHN dataset.

F Sigmoid activation

Note that when employing Sigmoid activation, after a certain scale the hidden layer gradients start to vanish. We try to compensate for this by increasing the number of hidden units to 2048.

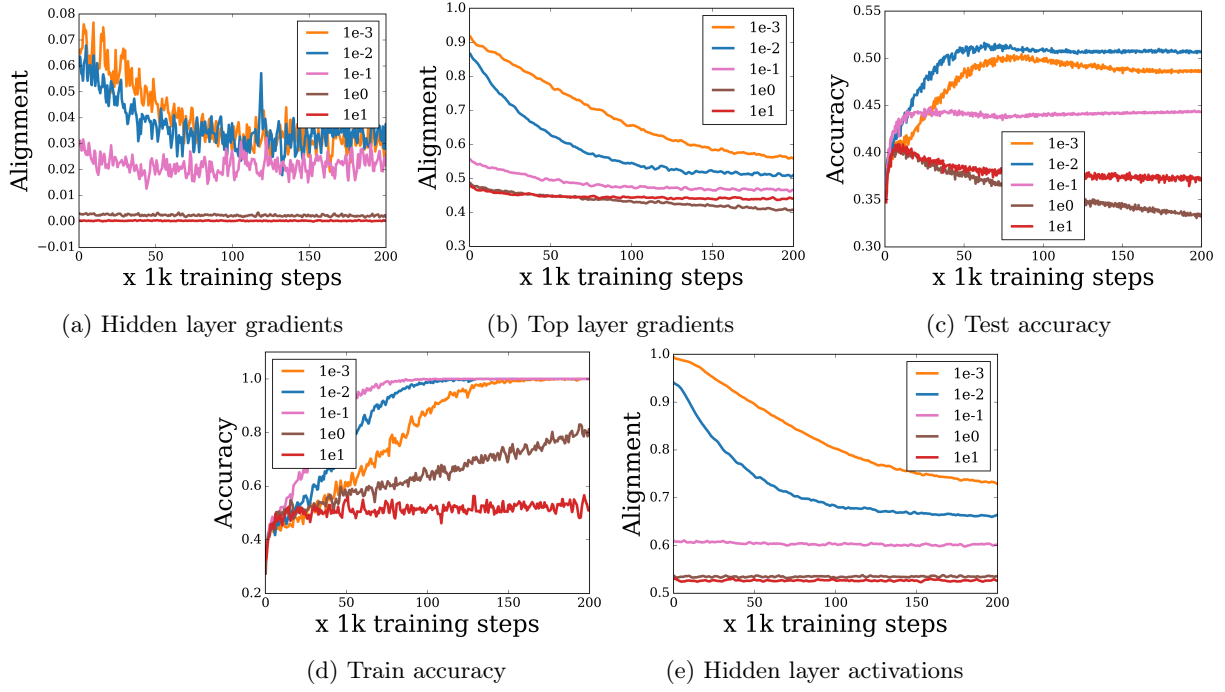


Figure 21: Results when using Sigmoid activation function on CIFAR10 dataset.

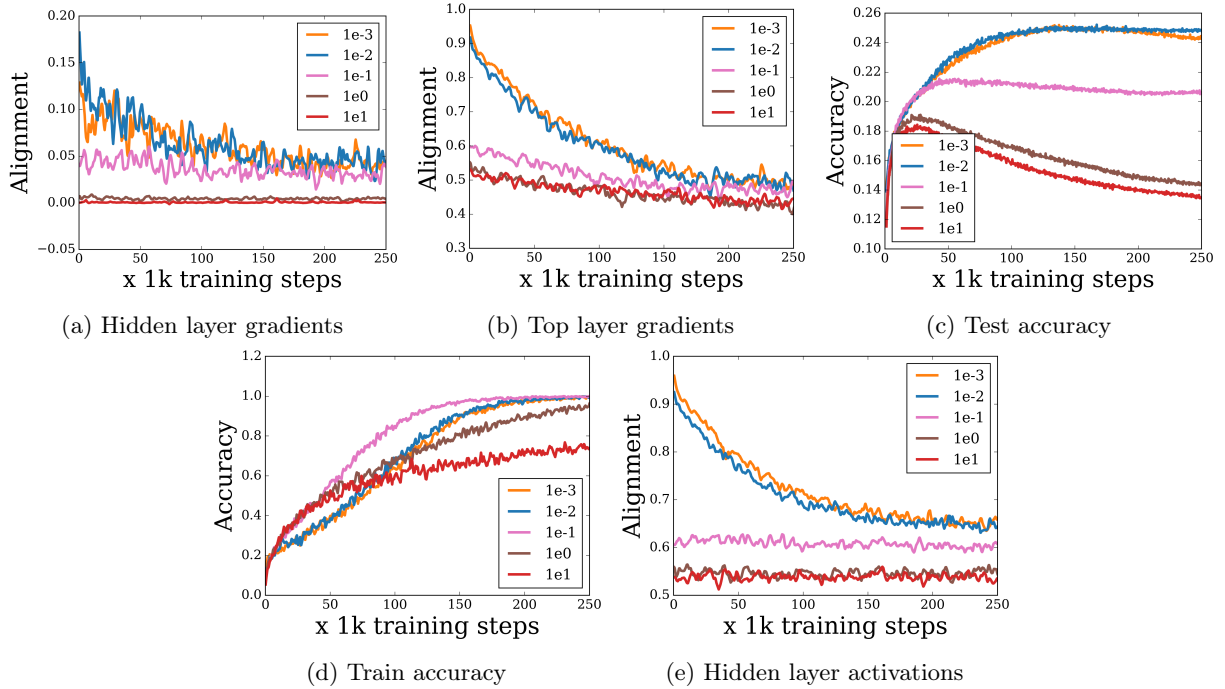


Figure 22: Results when using Sigmoid activation function on CIFAR100 dataset.

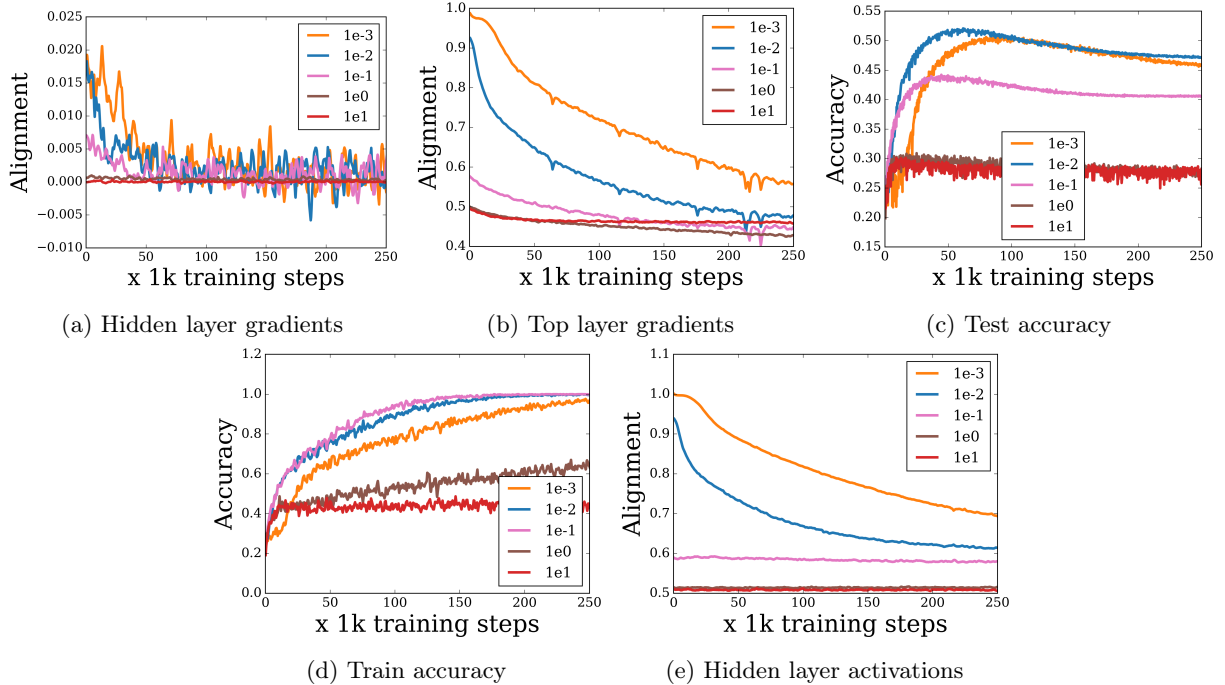


Figure 23: Results when using Sigmoid activation function on SVHN dataset.

G ConvNet architecture

Our goal is to recover the phenomenon that convolution and pooling operation leads to more aligned representations. In order to do this, we construct a simple ConvNet architecture. We start with two consecutive convolution and max pool operations, followed by a fully-connected and softmax layers. Note that the last two layers fully connected and softmax are operationally the same as our 2-layer MLP. We keep all the other hyper parameters the same between training runs for both the architectures. Both are trained with SGD without momentum with learning rate set to 0.01 and batch size to 256.

- Convolution layer 1: 32 filters with 5x5 kernel size followed by ReLU activation.
- Max pooling layer 1: pool size 3x3 with stride of 2x2
- Convolution layer 2: 64 filters with 5x5 kernel size followed by ReLU activation.
- Max pooling layer 2: pool size 3x3 with stride of 2x2
- Fully connected layer with 1024 hidden units followed by ReLU activation.
- Softmax layer with 10 output logits.